

Research



Cite this article: Zhang HH, Qin CK, Chen Y, Zhang Z. 2019 Inhibition behaviour of mild steel by three new benzaldehyde thiosemicarbazone derivatives in 0.5 M H₂SO₄: experimental and computational study. *R. Soc. open sci.* **6**: 190192. <http://dx.doi.org/10.1098/rsos.190192>

Received: 7 February 2019

Accepted: 22 July 2019

Subject Category:

Chemistry

Subject Areas:

chemical physics

Keywords:

inhibition, mild steel, EIS, theoretical calculation, acid corrosion

Author for correspondence:

Y. Chen

e-mail: chen123yu123@163.com

This article has been edited by the Royal Society of Chemistry, including the commissioning, peer review process and editorial aspects up to the point of acceptance.



Inhibition behaviour of mild steel by three new benzaldehyde thiosemicarbazone derivatives in 0.5 M H₂SO₄: experimental and computational study

H. H. Zhang^{1,3}, C. K. Qin², Y. Chen¹ and Z. Zhang³

¹Department of Chemical Engineering and Safety, and ²College of Aeronautical Engineering, Binzhou University, Binzhou, Shandong 256600, People's Republic of China

³Department of Chemistry, Zhejiang University, Hangzhou, Zhejiang 310027, People's Republic of China

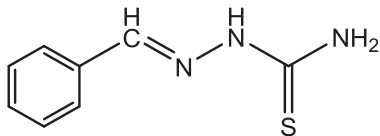
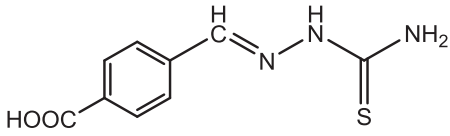
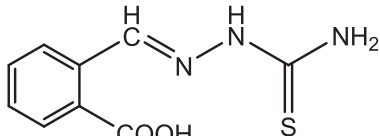
YC, 0000-0002-4169-039X

Three new benzaldehyde thiosemicarbazone derivatives namely benzaldehyde thiosemicarbazone (BST), 4-carboxyl benzaldehyde thiosemicarbazone (PBST) and 2-carboxyl benzaldehyde thiosemicarbazone (OCT) were synthesized and their inhibition effects on mild steel corrosion in 0.5 M H₂SO₄ solution were studied systematically using gravimetric and electrochemical measurements. Weight loss results revealed that PBST exhibited the highest inhibition efficiency of 96.6% among the investigated compounds when the concentration was 300 μM. The analysis of polarization curves indicated that the three benzaldehyde thiosemicarbazone derivatives acted as mixed type inhibitors and PBST and OCT predominantly anodic. The adsorption process of all these benzaldehyde thiosemicarbazone derivatives on Q235 steel surface in 0.5 M H₂SO₄ solution conformed to Langmuir adsorption isotherm. Scanning electron microscopy was conducted to show the presence of benzaldehyde thiosemicarbazone derivatives on Q235 mild steel surface. The results of theoretical calculations were in good agreement with that of experimental measurements.

1. Introduction

Mild steel has been applied as a popular construction material in petroleum, food, chemical and engineering industries [1–3].

Table 1. Physical and chemical properties of the synthesized compounds.

no.	molecular structure	abbreviations	structure characterizations
1		BST	C ₈ H ₉ N ₃ S (mol. wt. 179) M.P. 164–165°C IR spectrum (KBr, cm ⁻¹) 3399, 3144, 1599, 1283, 1098
2		PBST	C ₉ H ₉ O ₂ N ₃ S (mol. wt. 223) M.P. 197–199°C IR spectrum (KBr, cm ⁻¹) 3482, 3148, 1613, 1277, 1092
3		OCT	C ₉ H ₉ O ₂ N ₃ S (mol. wt. 223) M.P. 203–205°C IR spectrum (KBr, cm ⁻¹) 3173, 1606, 1270, 1105

However, mild steel is easily corroded in acidic solutions when they are serving in industrial washing, acid de-scaling and oil well acidization [4–6], which may cause significant economic losses and security risks. The use of inhibitors to prevent or minimize the considerable damage of mild steel in acid environment has been found to be one of the most economical and efficient methods [7–10]. It is generally believed that organic compounds containing heteroatoms such as nitrogen, oxygen and sulfur, or their molecular structure containing heterocyclic rings or polar functional groups serve as excellent organic inhibitors in acidic media [10]. The reason is that these compounds can form a strong chemical bond with the metal on the solid/liquid surface through charge transfer [11–13] and block the active site on the mild steel surface, thereby resisting the corrosion of mild steel in corrosive environment [14–17].

Gravimetric measurements [18,19], potentiodynamic polarization curves [20–22] and electrochemical impedance spectroscopy (EIS) [23–26] are classical methods to evaluate the inhibition behaviour. Theoretical calculation is a powerful technique to establish the relationship between the inhibition behaviour and molecular structure [27–29], which is helpful for designing a more effective inhibitor molecule. Moreover, some useful parameters, including the energy of the highest occupied molecular orbital, the energy of the lowest unoccupied molecular orbital, the energy gap and dipole moment can supply important information about the inhibition mechanism.

The objective of the present work is to investigate the inhibition behaviour of Q235 mild steel in 0.5 M H₂SO₄ solution containing three new synthesized benzaldehyde thiosemicarbazone derivatives namely benzaldehyde thiosemicarbazone (BST), 4-carboxyl benzaldehyde thiosemicarbazone (PBST) and 2-carboxyl benzaldehyde thiosemicarbazone (OCT) (table 1). The reason of choosing these compounds is that, firstly, these compounds contain various adsorption centres including oxygen, nitrogen and sulfur heteroatoms and -NH₂, -OH functional groups. Secondly, benzaldehyde thiosemicarbazone exhibited high inhibition efficiency for iron-base metallic glassy alloy in 0.5 M H₂SO₄ solution at 30°C, as previous reported [30]. Thirdly, these inhibitors can be easily synthesized with high yield. The study was carried out using weight loss measurement, potentiodynamic polarization curves, EIS and scanning electron microscopy (SEM). The correlation between the inhibition efficiencies of different substitution on the thiosemicarbazone compounds is discussed. Moreover, theoretical calculations were conducted to evaluate the inhibition mechanism.

2. Methods

2.1. Materials

The studied benzaldehyde thiosemicarbazone derivatives were synthesized according to the literature [30,31] and the chemical reaction equation is shown in figure 1. Table 1 depicts the physical and chemical properties of the synthesized compounds.

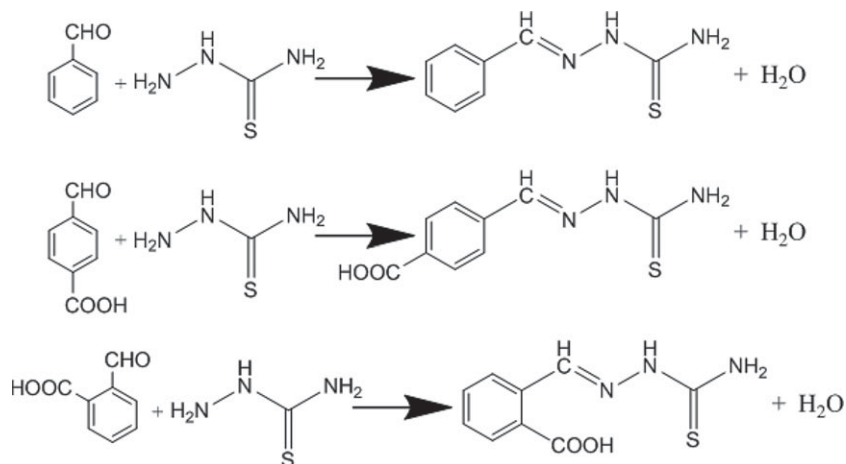


Figure 1. Chemical reaction equation of the studied compounds.

Table 2. Chemical composition (mass fraction, wt%) of Q235 mild steel samples.

C	Mn	Si	S	P	Fe
0.16	0.53	0.30	<0.055	<0.045	Bal.

2.2. Weight loss measurements

Weight loss experiments were performed in 500 ml 0.5 M H_2SO_4 solution containing different concentrations of benzaldehyde thiosemicarbazone derivatives. The testing time is 8 h at 298 K. Square specimens of Q235 carbon steel having dimensions $50 \times 25 \times 5$ mm were used for the gravimetric tests. The chemical composition of Q235 carbon steel is shown in table 2. The Q235 specimens were accurately weighed after degreasing with acetone and drying in N_2 . After 8 h corroding time, the Q235 samples were moved out and the surface was scrubbed with a bristle brush, and then weighed again. For each case, at least triplicate experiments were conducted and the average results are reported.

The corrosion rate for Q235 mild steel was derived from the following expression [32]:

$$\text{CR} = \frac{87.6 \times W}{A \times t \times \rho}, \quad (2.1)$$

where W is the mass loss of Q235 mild steel without and with addition of inhibitors in milligrams, A equals 32.5 cm^2 in our experimental condition, t is the testing time of 8 h, ρ is the Q235 mild steel density of 7.86×10^3 .

Thus, the inhibition efficiency (IE%) and surface coverage (θ) can be obtained from the corrosion rate using the following equation [32]:

$$\text{IE}(\%) = \left(1 - \frac{\text{CR}_{\text{inhi}}}{\text{CR}_{\text{free}}}\right) \times 100 \quad (2.2)$$

and

$$\theta = 1 - \frac{\text{CR}_{\text{inhi}}}{\text{CR}_{\text{free}}}, \quad (2.3)$$

where CR_{inhi} and CR_{free} are the obtained corrosion rates of Q235 mild steel with and without benzaldehyde thiosemicarbazone derivatives in 0.5 M H_2SO_4 solution, respectively.

2.3. Potentiodynamic polarization studies

The electrochemical measurements were carried out in a cylindrical glass cell of 250 ml with traditional three electrodes. A saturated calomel electrode (SCE) and a large platinum foil were employed as reference and counter electrode, respectively. Cylindrical Q235 mild steel sealed with Teflon was used

as working electrode and the exposed area was 0.50 cm². The exposed surface was abraded with fine sand paper and then polished to mirror using 2.5 μm diamond paste, cleaned with double-distilled water and finally immersed into the electrochemical glass cell containing 0.5 M H₂SO₄ solution without and with different concentrations of benzaldehyde thiosemicarbazone derivatives for at least 1 h. When the open circuit potential (E_{ocp}) reached a steady state, the potentiodynamic polarization study was performed using CHI660A electrochemical workstation at a scan rate of 1 mV s⁻¹. The scanning potential ranges from $E_{ocp} - 250$ mV to $E_{ocp} + 250$ mV. Tafel extrapolation method was employed to obtain some useful parameters, including corrosion potential (E_{corr}), corrosion current density (j_{corr}), anodic and cathodic Tafel slopes. The inhibition efficiency η_p (%) is then derived from the corrosion current density as follows:

$$\eta_p \% = \left(1 - \frac{j_{inhi}}{j_{free}}\right) \times 100\%, \quad (2.4)$$

where j_{inhi} and j_{free} are the obtained corrosion current densities with and without BST, PBST and OCT inhibitors, respectively.

2.4. Electrochemical impedance experiments

EIS was conducted using PARSTAT 2273 measurement unit in the frequency range of 10 mHz–100 kHz at E_{ocp} and the scanning always initiated from high frequency to low frequency. The voltage amplitude was 5 mV. Each concentration was repeatedly tested three times or more and the average results were calculated. The EIS experimental data was analysed using Z-View software. The inhibition efficiency η_{EIS} (%) can be obtained from the charge transfer resistance as follows:

$$\eta_{EIS} \% = \frac{R_{ct} - R_{ct}^0}{R_{ct}}, \quad (2.5)$$

where R_{ct}^0 and R_{ct} are the charge transfer resistance for Q235 mild steel in uninhibited and inhibited solution, respectively.

2.5. Scanning electron microscopy measurements

The Q235 mild steel surface after corroded in 0.5 M H₂SO₄ solution at 298 K without and with inhibitors was observed with SEM model Hitachi SU80 instrument at an accelerating voltage of 5 kV at 2000× magnification. EDX detector model coupled with SEM was used to evaluate the surface composition of Q235 mild steel.

2.6. Theoretical calculations

As described in previous literature [33,34], the geometric optimizations of the synthesized derivatives and quantum chemical calculations were performed using the functional hydride B3LYP density functional theory (DFT) formalism. During the calculations, the electron basis set 6-31G (d, p) in the standard Gaussian-03 software package was employed. As a result, some useful quantum chemical parameters, such as energy of the lowest unoccupied molecular orbital (E_{LUMO}), the energy of the highest occupied molecular orbital (E_{HOMO}), the energy gap (ΔE) between LUMO and HOMO, the ionization potential (I), the electron affinity (A), dipole moment, the global hardness (η) and the global softness (σ) were calculated.

3. Results and discussion

3.1. Weight loss tests

The inhibitive effect of the synthesized benzaldehyde thiosemicarbazone derivatives (BST, PBST and OCT) for Q235 mild steel in 0.5 M H₂SO₄ solution at 298 K was initially investigated with weight loss measurements. The calculated values of corrosion rate, inhibition efficiency and surface coverage are summarized in table 3. Obviously, the corrosion rate decreased considerably with addition of these compounds compared to the blank, which may be related to the strong adsorption of these compounds onto Q235 mild steel surface and forming a protective physical barrier to resist the acid

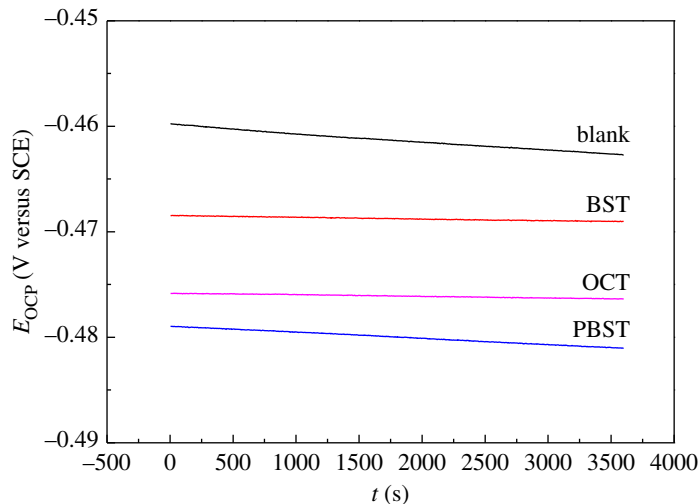


Figure 2. Open circuit potential for Q235 mild steel in 0.5 M H_2SO_4 solution without and with 300 μM BST, PBST and OCT inhibitor.

Table 3. The weight loss parameters for Q235 steel in 0.5 M H_2SO_4 containing different concentrations of BST, PBST and OCT inhibitor at 298 K.

inhibitor	C_{inh} (μM)	CR ($\text{mg cm}^{-2} \text{h}^{-1}$)	η (%)	θ
blank	0	6.09	—	
BST	50	2.75	54.8	0.548
	100	1.71	71.9	0.719
	200	1.12	81.6	0.816
	300	0.87	85.7	0.857
PBST	50	2.33	61.7	0.617
	100	1.24	79.6	0.796
	200	0.66	89.2	0.892
	300	0.21	96.6	0.966
OCT	50	2.11	65.4	0.654
	100	1.37	77.5	0.775
	200	0.76	87.5	0.875
	300	0.40	93.4	0.934

attack [35]. It is clear that with increasing the inhibitor concentration, the inhibition efficiency also increased and the highest value was found to be 85.7%, 96.6% and 93.4% for BST, PBST and OCT compounds, respectively at 300 μM , suggesting that these inhibitors effectively inhibited the Q235 mild steel corrosion in acidic medium. It can also be deduced from table 3 that at the same concentration, the inhibition efficiency follow the order: PBST > OCT > BST, indicating that PBST exhibits the best inhibitive performance compared to other two benzaldehyde thiosemicarbazone derivatives. This result may be correlated with its molecular structure of $-\text{COOH}$ functional group at the ρ -substitution (table 1).

3.2. Open circuit potential curves

The open circuit potential for Q235 mild steel in 0.5 M H_2SO_4 solution without and with 300 μM BST, PBST and OCT inhibitor is depicted in figure 2. It can be seen that the OCP reached a steady state after 1 h immersion time. Apparently, the OCP value moved in the negative direction with addition of 300 μM BST, PBST and OCT inhibitor compared to the blank. This shift may be correlated to the adsorption of these compounds on mild steel surface.

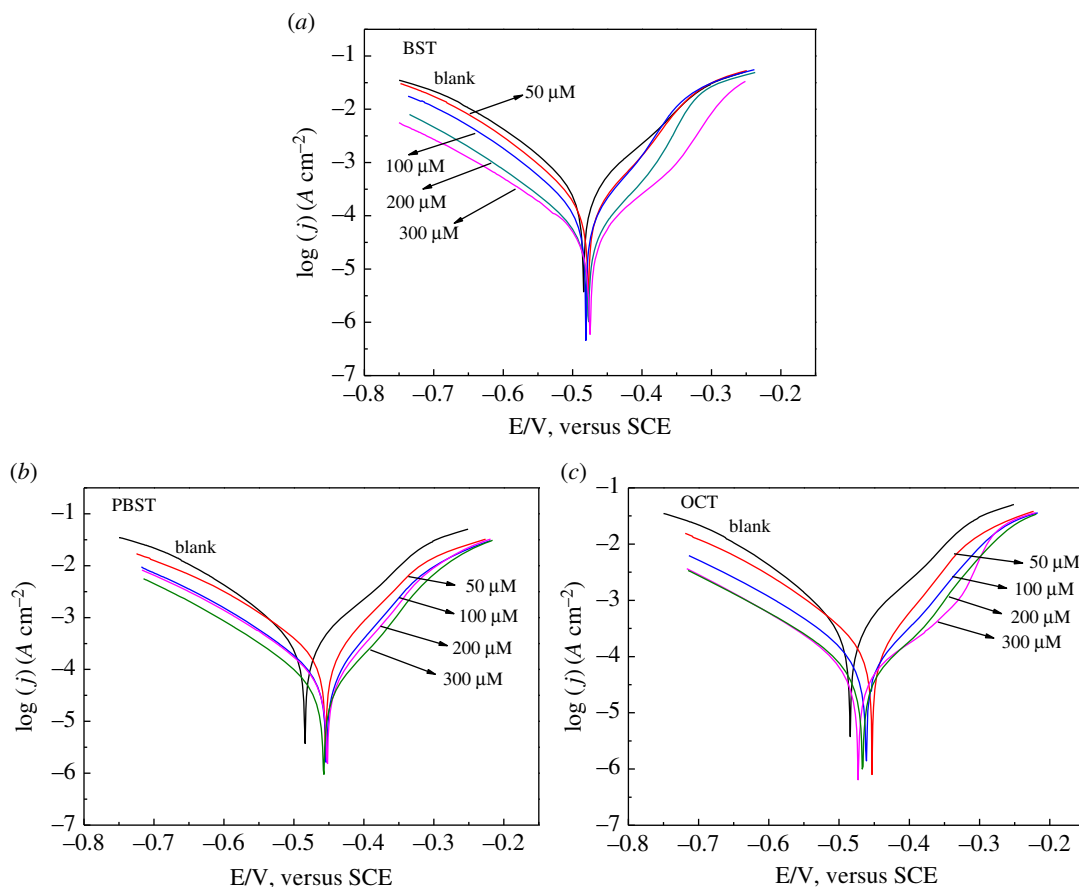


Figure 3. Polarization curves for Q235 mild steel in 0.5 M H_2SO_4 solution containing different concentrations of (a) BST, (b) PBST and (c) OCT inhibitor.

3.3. Potentiodynamic polarization curves

Figure 3 shows the polarization curves for Q235 mild steel in 0.5 M H_2SO_4 solution containing different concentrations of BST, PBST and OCT inhibitor. Apparently, the current densities of both the anodic and cathodic branches decreased with addition of benzaldehyde thiosemicarbazone derivatives, indicating that both the anodic and cathodic reaction rates were resisted which was generally due to the adsorption of these inhibitors at the active sites on the surface. It is noticeable that the shape of polarization curves without inhibitors is similar to that with addition of these three inhibitors. This phenomenon demonstrated that the addition of these inhibitors did not change the corrosion mechanism of Q235 mild steel dissolution in 0.5 M H_2SO_4 solution [36] and the inhibitive effect of these inhibitors is originated from the coverage of inhibitor molecules at the active sites to restrain their exposure to the acidic environment. In addition, it can be seen that there was no obvious trend observed in the E_{corr} values for BST inhibitor compared to the blank, which moves to the positive direction with less than 85 mV in the presence of PBST and OCT inhibitors, suggesting that these inhibitors were of mixed type and PBST and OCT predominantly anodic [37–39]. The values of E_{corr} , j_{corr} , cathodic and anodic Tafel slopes, and η_p (%) are listed in table 4. Obviously, j_{corr} values decreased remarkably with addition of these inhibitors compared to the uninhibited. With increasing inhibitors concentration from 0 to 300 μM , the values of j_{corr} decreased from 375.8 $\mu\text{A cm}^{-2}$ to 50.2, 34.8 and 36.1 $\mu\text{A cm}^{-2}$ for BST, PBST and OCT inhibitors, respectively. Therefore, η_p exhibited a maximum value of 87.1%, 90.7% and 90.4% for BST, PBST and OCT inhibitor, respectively. Observation of table 4 shows that the inhibition efficiency obeys the order: PBST > OCT > BST, which is in good accordance with the gravimetric tests.

3.4. Electrochemical impedance spectroscopy measurements

The representative Nyquist plots for Q235 mild steel dissolution in 0.5 M H_2SO_4 solution at 298 K in the absence and presence of different concentrations of BST, PBST and OCT inhibitors are shown in figure 4. It is apparent that the Nyquist plots were considerably influenced after the addition of these

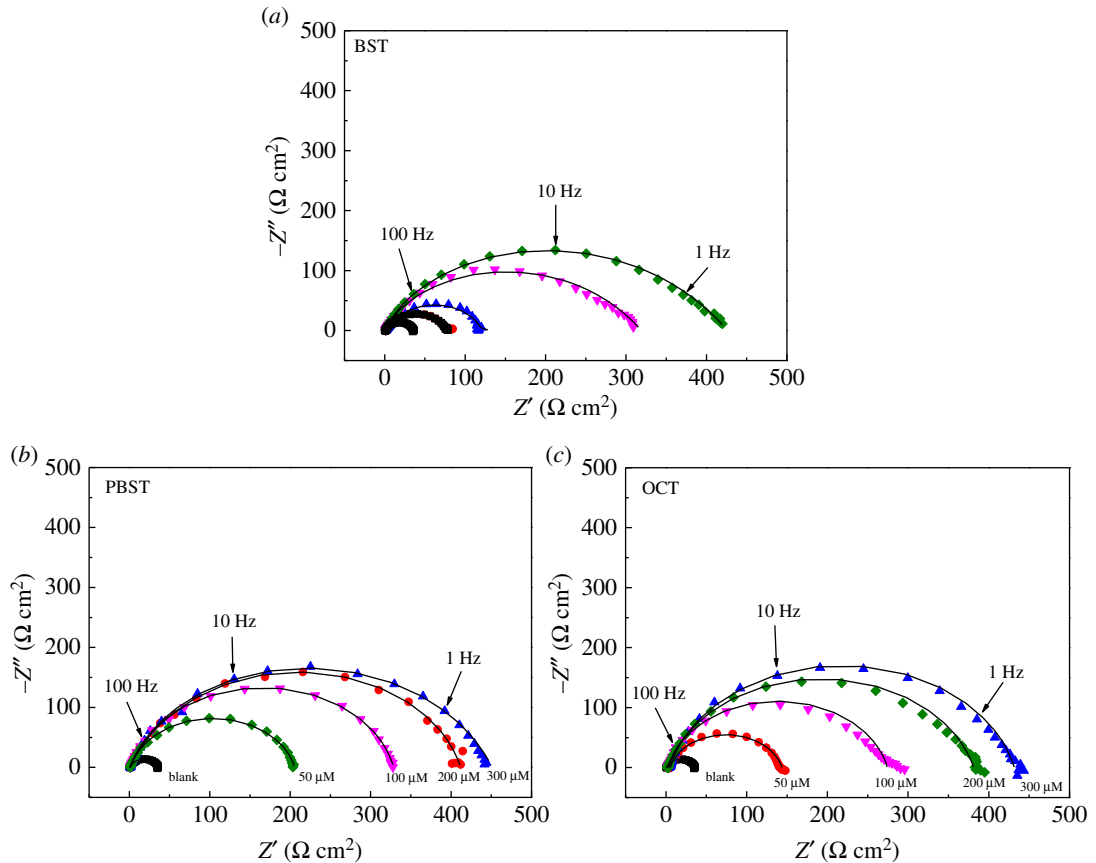


Figure 4. Nyquist plots for Q235 mild steel corrosion in 0.5 M H_2SO_4 solution at 298 K containing different concentrations of (a) BST, (b) PBST and (c) OCT.

Table 4. Polarization parameters for Q235 mild steel corroded in 0.5 M H_2SO_4 containing different concentrations of BST, PBST and OCT inhibitor at 298 K.

inhibitor	C_{inh} (μM)	E_{corr} (mV)	β_a (mV dec^{-1})	$-\beta_c$ (mV dec^{-1})	j_{corr} ($\mu\text{A cm}^{-2}$)	η_p (%)
blank	0	-479.1	113.9	102.4	375.8	
BST	50	-477.2	119.5	105.0	218.5	41.9
	100	-479.9	121.5	102.6	122.9	67.3
	200	-478.8	116.7	97.7	54.1	85.6
	300	-475.6	109.0	100.2	50.2	87.1
PBST	50	-457.1	102.9	110.1	167.3	55.5
	100	-448.6	105.2	108.3	67.2	82.1
	200	-458.8	98.6	110.4	51.9	86.2
	300	-460.4	100.4	108.2	34.8	90.7
OCT	50	-456.2	98.4	126.8	198.6	47.1
	100	-450.6	102.1	124.3	90.6	75.9
	200	-455.8	98.3	112.9	53.0	85.8
	300	-459.3	100.9	121.5	36.1	90.4

inhibitors into 0.5 M H_2SO_4 solution, which diameter was greater than that in the blank solution, suggesting that the Q235 mild steel dissolution process was remarkably restrained by these inhibitors. As observed, for the uninhibited case, the impedance spectrum contains only one depressed capacitive loop, while after the addition of BST, PBST and OCT inhibitors, the Nyquist plots show

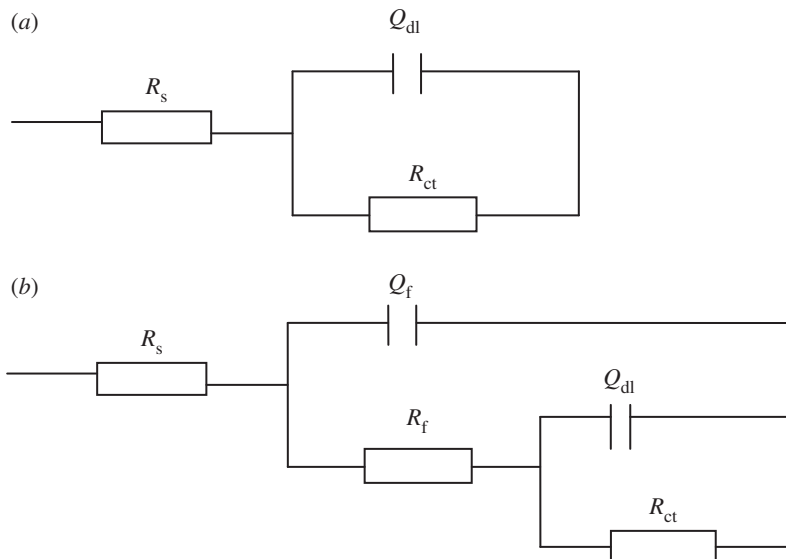


Figure 5. EEC model used to simulate the EIS data. (R_s : solution resistance, Q_{dl} : double layer capacitance; R_{ct} : charge transfer resistance; Q_f : film capacitance; R_f : film resistance).

Table 5. EIS parameters for Q235 mild steel in 0.5 M H_2SO_4 containing different concentrations of BST, PBST and OCT inhibitor.

	C_{inh} (μM)	R_s (Ωcm^2)	Q_f ($\Omega^{-1} s^n cm^{-2}$)	R_f (Ωcm^2)	R_{ct} (Ωcm^2)	Q_{dl} ($\Omega^{-1} s^n cm^{-2}$)	n_{dl}	η_{EIS} (%)
blank	0	0.88 ± 0.02			33.4 ± 1.1	175 ± 6.1	0.968	—
BST	50	1.05 ± 0.03	242 ± 10	2.16 ± 0.08	78.4 ± 1.8	84.6 ± 4.3	1	57.4
	100	0.99 ± 0.03	206 ± 8	2.44 ± 0.04	126.9 ± 3.2	72.2 ± 2.0	1	73.7
	200	1.02 ± 0.02	169 ± 4	12.1 ± 0.16	306.4 ± 8.3	56.6 ± 2.2	0.945	89.1
	300	1.02 ± 0.03	132 ± 5	16.8 ± 0.12	408.9 ± 7.6	51.4 ± 3.1	0.922	91.8
PBST	50	1.08 ± 0.02	213 ± 7	9.24 ± 0.14	175.6 ± 5.2	73.6 ± 3.5	0.948	80.9
	100	0.93 ± 0.02	182 ± 5	11.2 ± 0.16	252.3 ± 4.9	71.4 ± 2.4	0.916	86.7
	200	0.96 ± 0.03	130 ± 3	13.6 ± 0.12	371.6 ± 8.2	46.4 ± 1.3	0.953	91.0
	300	0.89 ± 0.02	114 ± 2	17.4 ± 0.23	485.3 ± 7.1	32.2 ± 0.9	0.942	93.2
OCT	50	0.84 ± 0.03	225 ± 6	3.58 ± 0.11	113.4 ± 2.6	84.6 ± 1.7	0.974	70.5
	100	1.03 ± 0.02	196 ± 4	6.26 ± 0.15	242.2 ± 5.6	58.2 ± 1.3	0.906	86.2
	200	1.06 ± 0.02	143 ± 3	11.4 ± 0.12	356.5 ± 8.2	41.2 ± 1.2	0.930	90.6
	300	0.97 ± 0.03	128 ± 4	15.7 ± 0.14	460.8 ± 11	24.8 ± 0.8	0.961	92.8

two capacitive loops which may correspond to the double electric layer and film capacitance, respectively. Obviously, the diameter of the capacitive loops became larger with the increase of inhibitor concentration. Figure 3 also shows that the centres of the impedance loops are below the real axis. This finding indicates a non-ideal electrochemical behaviour at the metal/solution interface [40,41], which generally resulted from the surface roughness and heterogeneities [42,43]. Therefore, a constant phase element CPE (Q) was used to replace capacity [44] and the thus improved electrochemical equivalent circuit (EEC) is depicted in figure 4, which was used to analyse the EIS data. The admittance of a CPE can be calculated using the following expression [45]:

$$Y_{CPE} = Y_0(j\omega)^n, \quad (3.1)$$

where Y_0 is the magnitude, j equals -1 , ω is the angular frequency, and n is the phase shift, representing the surface inhomogeneity [46] (figure 5).

The fitted results are summarized in table 5. It can be seen that the values of R_{ct} increased upon rising of inhibitors concentration, suggesting a higher corrosion resistance by the adsorption of these inhibitors onto

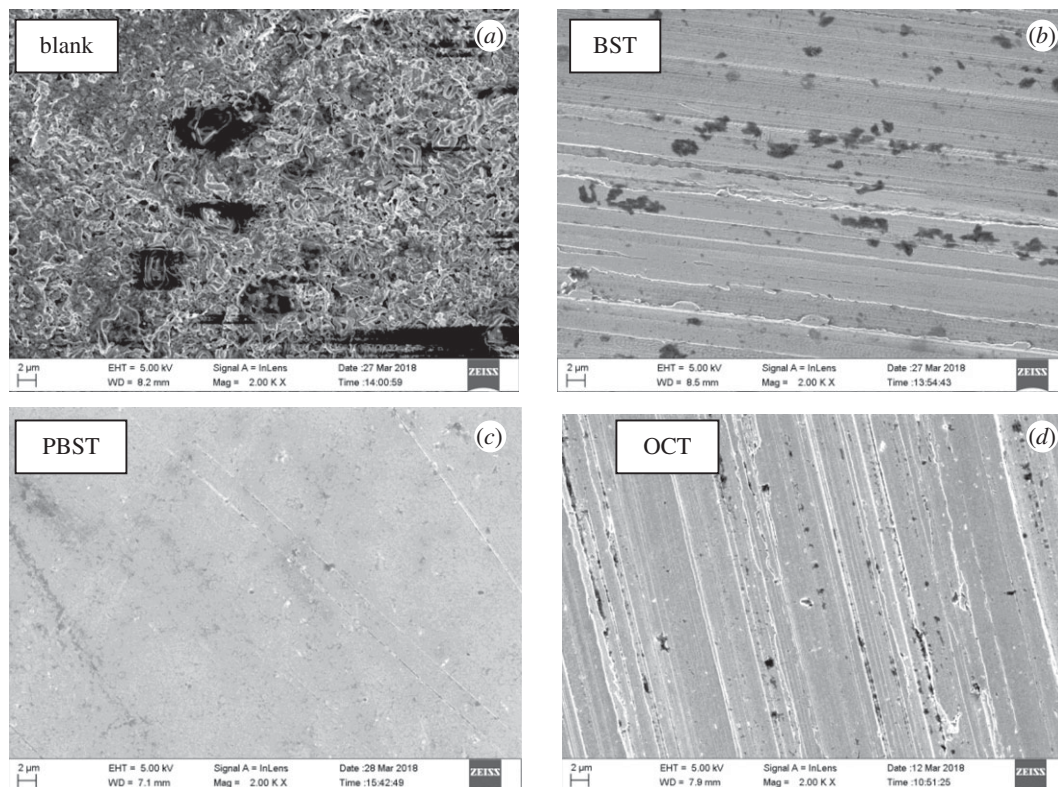


Figure 6. Surface morphology of Q235 mild steel after being corroded in 0.5 M H_2SO_4 solution at 298 K in the absence (a) and presence of 300 μM (b) BST, (c) PBST and (d) OCT.

Q235 mild steel surface. The R_{ct} values reached 408.9, 485.3 and 460.8 $\Omega \text{ cm}^2$ for BST, PBST and OCT inhibitors respectively, when their concentration was 300 μM . Accordingly, the inhibition efficiency exhibited a maximum value of 91.8%, 93.2% and 92.8% for BST, PBST and OCT, respectively. Oppositely, the Q_{dl} values decreased with the increase of inhibitors concentration. The reason may be that the synthesized benzaldehyde thiosemicarbazone derivatives adsorbed on the metal surface and formed a stronger chemical bond with steel than water molecules, thus the previously absorbed water molecules were replaced [47,48]. Additionally, the values of n were all near to 1 in the absence and presence of these inhibitors (table 5), suggesting the homogeneous nature of the surface. Moreover, it is worth noting that the inhibition efficiencies of PBST and OCT inhibitor are higher than that of BST at the same concentration, which may be correlated to the presence of $-\text{COOH}$ functional group in the molecular structure.

3.5. Surface investigation

SEM images of Q235 mild steel samples after being corroded in 0.5 M H_2SO_4 solution without and with addition of 300 μM BST, PBST and OCT inhibitors are shown in figure 6. It is observed that the Q235 mild steel surface was strongly damaged without inhibitors (figure 6a), while the surface was smooth and compact when 300 μM inhibitors was added (figure 6b–d), indicating that benzaldehyde thiosemicarbazone derivatives formed a protective physical barrier on the mild steel surface and retarded the aggressive acid attack. The presence of these inhibitors was further confirmed by EDX spectra, as shown in figure 7. It is worth noting that no characteristic peaks for nitrogen (N) and sulfur (S) can be found in the uninhibited solution (figure 7a), whereas both of them appeared on Q235 mild steel surface in 0.5 M H_2SO_4 solution containing 300 μM inhibitors (figure 7b–d), which indicated the presence of these inhibitor molecules to form a protective film on the Q235 mild steel surface. Moreover, the percentage atomic contents of elements obtained from EDX measurements for Q235 mild steel samples in the absence and presence of 300 μM BST, PBST and OCT is given in table 6. It also can be seen that the percentage atomic content of Fe reduced sharply with addition of 300 μM BST, PBST and OCT inhibitors compared to the blank, which was due to the surface coverage of these inhibitor molecules on Q235 mild steel surface.

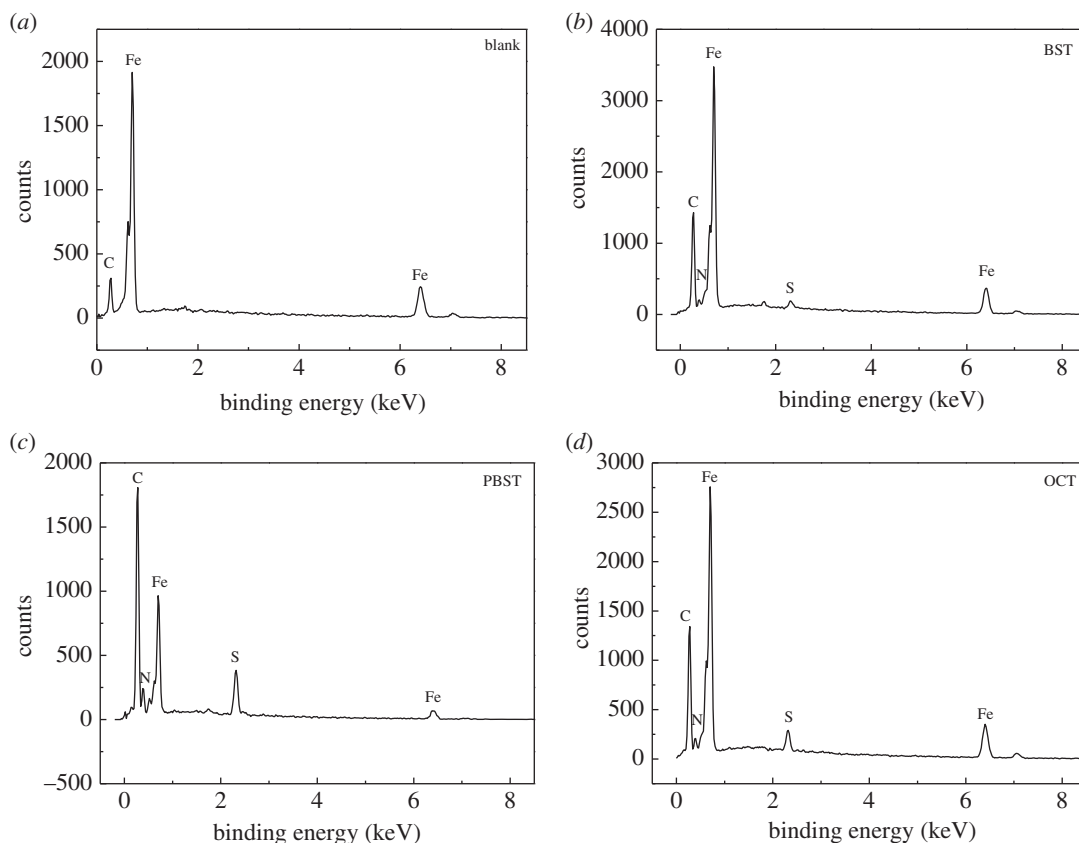


Figure 7. EDX spectra of Q235 mild steel surface in 0.5 M H_2SO_4 at 298 K in the absence (a) and presence of 300 μM (b) BST, (c) PBST and (d) OCT.

Table 6. EDX spectra results for mild steel samples in the absence and presence of 300 μM BST, PBST and OCT.

inhibitor	Fe	C	N	S
blank	70.78	29.22	—	—
BST	67.84	27.53	2.82	1.81
PBST	62.54	26.52	6.64	4.30
OCT	64.65	26.65	5.07	3.63

3.6. Adsorption isotherm

To further explore the adsorption mechanism of BST, PBST and OCT inhibitors onto Q235 mild steel in 0.5 M H_2SO_4 solution, different adsorption isotherms, including Langmuir, Flory-Huggins, Temkin, Freundlich and Frumkin isotherm models were employed. In the present study, a linear relationship between c/θ values and inhibitors concentration c was established, as shown in figure 8, which indicated that the adsorption of these inhibitors on Q235 mild steel surface in 0.5 M H_2SO_4 solution conformed to Langmuir adsorption isotherm with the following expression [49,50]:

$$\frac{c}{\theta} = \frac{1}{K_{\text{ads}}} + c, \quad (3.2)$$

where K_{ads} is the equilibrium constant of inhibitors adsorption onto Q235 mild steel surface, which values can be obtained from the intercept of figure 8. According to the relationship between the standard free energy of adsorption ΔG_{ads}^0 and K_{ads} , ΔG_{ads}^0 can be calculated from the value of K_{ads} using the following equation [51]:

$$K_{\text{ads}} = \frac{1}{55.5} \exp\left(\frac{-\Delta G_{\text{ads}}^0}{RT}\right), \quad (3.3)$$

where R is the molar gas constant and T is the absolute temperature. The calculated equilibrium constant K_{ads} and standard free energy of adsorption ΔG_{ads}^0 are summarized in table 7.

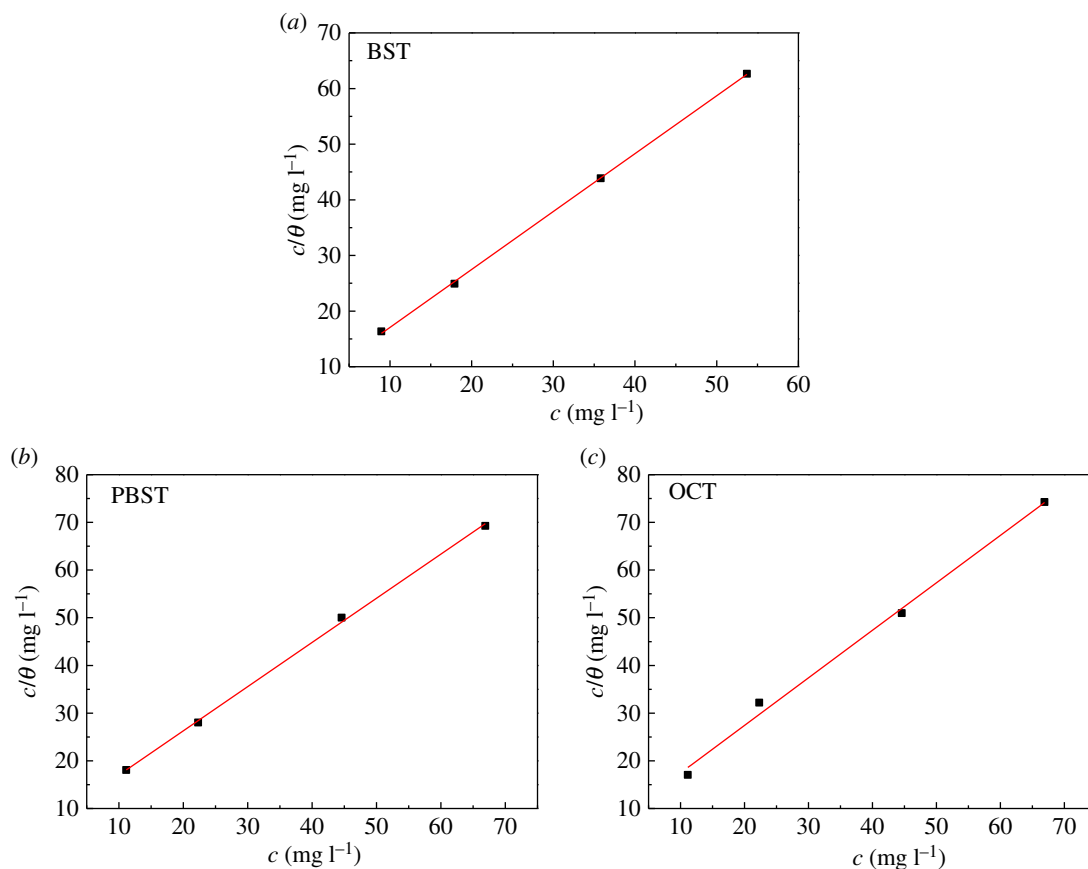


Figure 8. Langmuir isotherm for adsorption of (a) BST, (b) PBST and (c) OCT molecules onto Q235 mild steel in 0.5 M H₂SO₄ solution.

Table 7. The values of K_{ads} and ΔG_{ads}^0 for Q235 mild steel in the presence of BST, PBST and OCT inhibitors in 0.5 M H₂SO₄ solution.

inhibitor	$K_{\text{ads}}(\times 10^4/\text{M})$	ΔG_{ads}^0 (kJ mol ⁻¹)	slope	R^2
BST	2.62	-35.1	1.04	0.999
PBST	3.26	-35.7	0.98	0.999
OCT	2.97	-35.4	1.00	0.992

In our present measurements, the values of ΔG_{ads}^0 are found to be -35.1, -35.7 and -35.4 kJ mol⁻¹ for BST, PBST and OCT inhibitors, respectively. It is reported that the adsorption of organic inhibitor molecules onto metal surface follows physical adsorption through electrostatic interaction when the value of ΔG_{ads}^0 was positive to -20 kJ mol⁻¹, which conforms to chemisorptions involving charge sharing or charge transfer between the metal surface and inhibitor molecules when ΔG_{ads}^0 value was negative to -40 kJ mol⁻¹ [52–54]. Therefore, it is reasonable to deduce that the adsorption process of BST, PBST and OCT inhibitors onto Q235 mild steel surface is a combination of both chemisorptions and physisorption, which are predominant chemisorptions.

3.7. Effect of temperature

To further obtain the thermodynamic and activation parameters, weight loss experiments were performed at different temperatures ranging from 25°C to 55°C. The calculated corrosion rate and inhibition efficiency under different temperatures are listed in table 8. It is apparent that the corrosion rate increases with raising temperature for all these inhibitors. Meanwhile, the inhibition efficiency increases with temperature as well, which corresponds to the chemisorptions mechanism of inhibitor molecule onto metal surface. This phenomenon has been explained by the specific interaction between

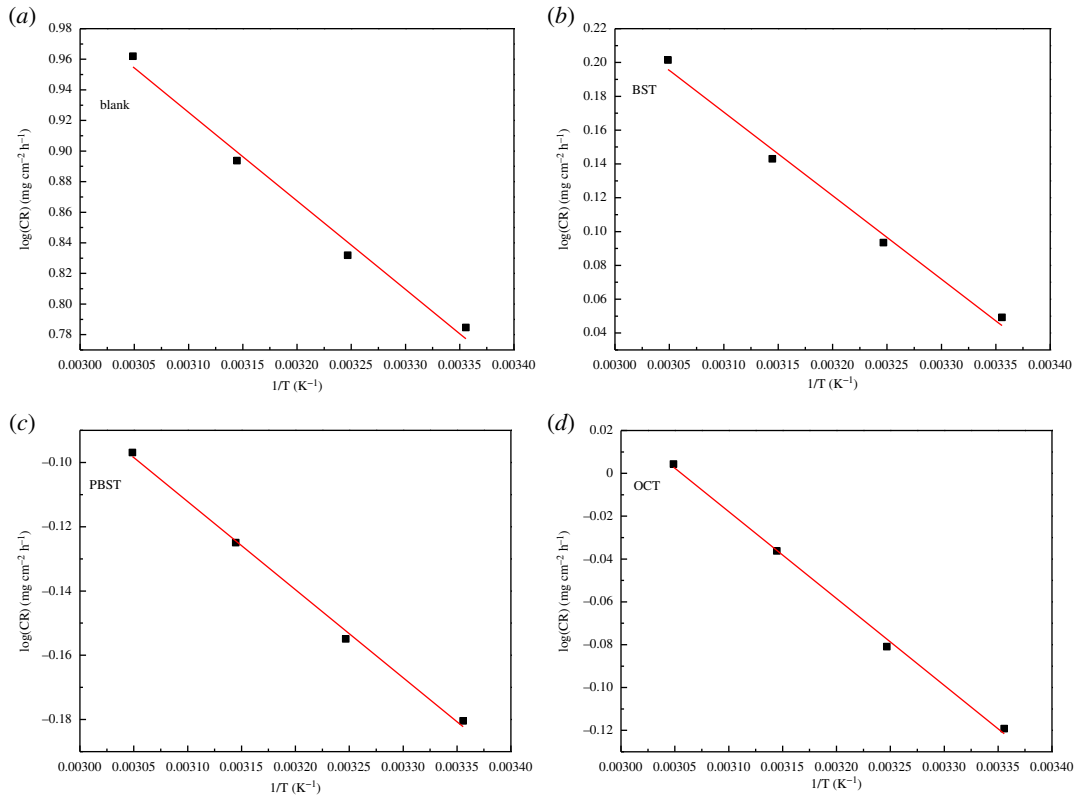


Figure 9. Log CR versus $1/T$ for Q235 mild steel in 0.5 M H_2SO_4 solution.

Table 8. Weight loss parameters for Q235 mild steel corroded in 0.5 M H_2SO_4 solution with addition of 200 μM BST, PBST and OCT inhibitors at different temperatures.

inhibitor	temperature (°C)	blank CR ($mg\ cm^{-2}\ h^{-1}$)	200 μM CR ($mg\ cm^{-2}\ h^{-1}$)	η (%)
BST	25	6.09	1.12	81.6
	35	6.79	1.24	81.7
	45	7.83	1.39	82.2
	55	9.16	1.59	82.6
PBST	25	6.09	0.66	89.2
	35	6.79	0.70	89.7
	45	7.83	0.75	90.4
	55	9.16	0.80	91.3
OCT	25	6.09	0.76	87.5
	35	6.79	0.83	87.8
	45	7.83	0.92	88.3
	55	9.16	1.01	90.0

inhibitor molecule and mild steel [55–58]. The apparent activation energy (E_a) is calculated by Arrhenius equation [59],

$$\log(CR) = \frac{-E_a}{2.303RT} + \log(A), \quad (3.4)$$

where E_a is the apparent activation energy and A is the Arrhenius pre-exponential factor.

The E_a values were obtained from the slope of Arrhenius plot as shown in figure 9 and the results are shown in table 9. It is obvious that E_a values for the Q235 mild steel dissolution in 0.5 M H_2SO_4 solution

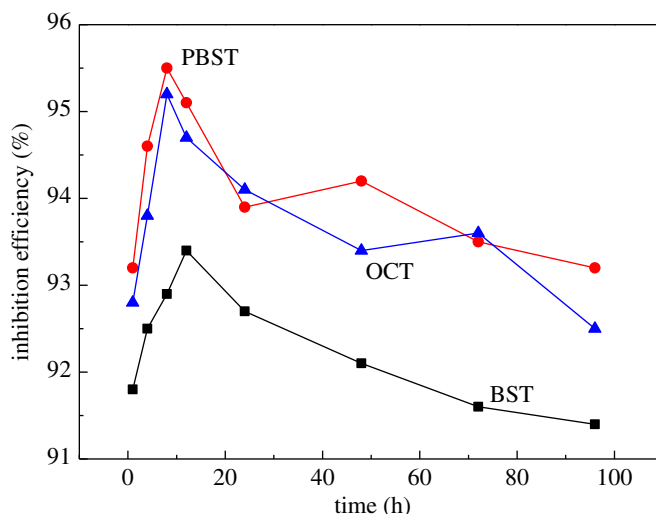


Figure 10. Effect of immersion time on the inhibition efficiency for 300 μM BST, PBST and OCT inhibitors onto Q235 mild steel in 0.5 M H_2SO_4 at 298 K.

Table 9. The apparent activation energy of mild steel corroded in 0.5 M H_2SO_4 without and with addition of 200 μM BST, PBST and OCT inhibitors.

inhibitor	E_a (KJ mol^{-1})
blank	11.1
BST	9.45
PBST	5.25
OCT	7.76

containing 200 μM inhibitors were smaller than that in the uninhibited. It was previously reported that the adsorption of organic inhibitor molecules follows chemisorptions mechanism when E_a value was unchanged or lower compared to the blank [37,60], which was explained by some of the energy being consumed in the chemical reaction. This finding furthermore supports the conclusion that was inferred from the Langmuir isotherm that the adsorption behaviour of the synthesized compounds on mild steel surface conforms to chemisorptions.

3.8. Effect of immersion time

The impact of immersion time on the inhibition efficiency for 300 μM BST, PBST and OCT inhibitors onto Q235 mild steel in 0.5 M H_2SO_4 solution at 298 K is shown in figure 10. It can be seen that during the initial 8 h, the inhibition efficiency increased with immersion time for PBST and OCT inhibitor, whereas 12 h for BST inhibitor, which may be correlated to the film growth and rearrangement of the BST, PBST and OCT inhibitor molecules on Q235 surface. After that, the inhibition efficiency decreased with prolonging immersion time, which may be linked to desorption or dissolution of adsorbed inhibitor molecules [61]. It is noticeable that during the whole testing immersion time, the inhibition efficiency of PBST and OCT inhibitors is higher than that of BST inhibitor. Moreover, the inhibition efficiencies of all these inhibitors were still over 90% after 96 h immersion time, suggesting that these synthesized inhibitors were all long-term effective inhibitors for Q235 mild steel in 0.5 M H_2SO_4 solution.

3.9. Quantum chemical calculations

To explore the correlation between the inhibition behaviour and molecular structures, the quantum chemical calculation were performed, and the optimized geometry structures and the frontier

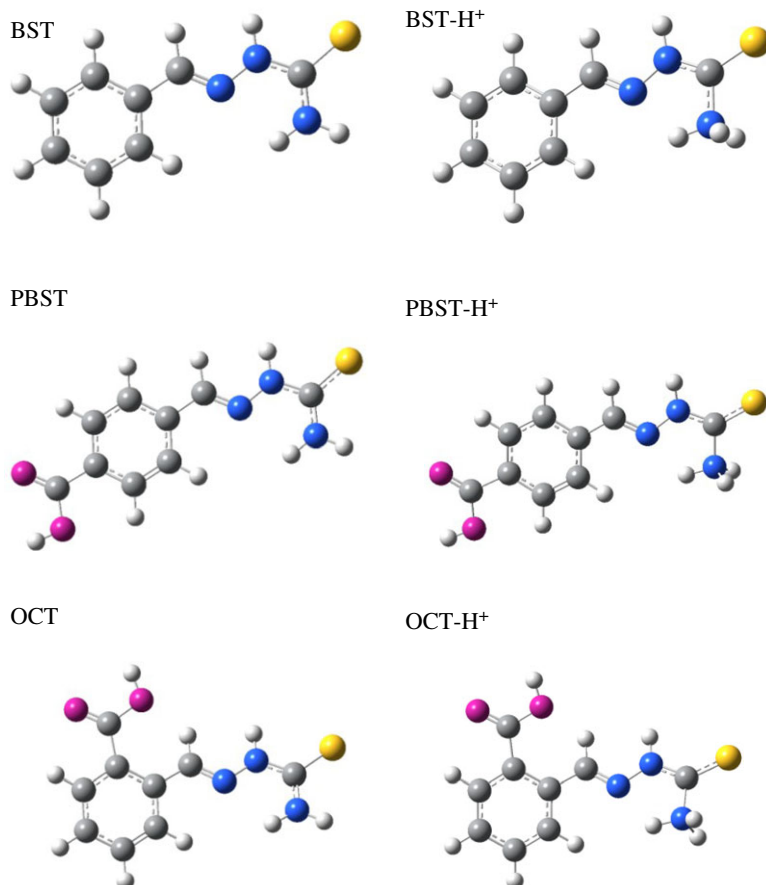


Figure 11. Optimized structure of BST, PBST and OCT and the protonated forms.

molecule orbital density distributions of these inhibitors as well as their protonated forms are presented in figures 11 and 12. The useful parameters, such as E_{HOMO} , E_{LUMO} , energy gap ΔE and dipole moment were determined and applied to explore the correlation between the inhibitor molecular structure and mild steel. According to the frontier molecular orbital theory, E_{HOMO} is related to the ability of a molecule to donate electrons to appropriate electron acceptors, thus, a molecule exhibits stronger tendency to donate electrons to the steel vacancy d-orbital in the present study when the calculated E_{HOMO} value is higher. Whereas, E_{LUMO} corresponds to the electron accepting ability of the molecule, and a molecule has higher capability of accepting electrons when the calculated E_{LUMO} value is lower [27,62,63]. Furthermore, the energy gap ΔE is an important parameter to evaluate the inhibitive effect of the inhibitor molecules. It was previously inferred [64,65] that an inhibitor possesses higher inhibition efficiency when its ΔE value is smaller, because lower energy is needed to remove an electron from the last occupied orbital.

According to Lukovits theorem [61], the value of ionization potential (I) and the electron affinity (A) can be derived from E_{LUMO} and E_{HOMO} by the following equations:

$$I = -E_{\text{HOMO}} \quad (3.5)$$

and

$$A = -E_{\text{LUMO}}. \quad (3.6)$$

Additionally, the absolute electronegativity (χ), the global hardness (ρ) and softness (σ) of the inhibitor molecule are defined as follows:

$$\chi = \frac{I - A}{2}, \quad (3.7)$$

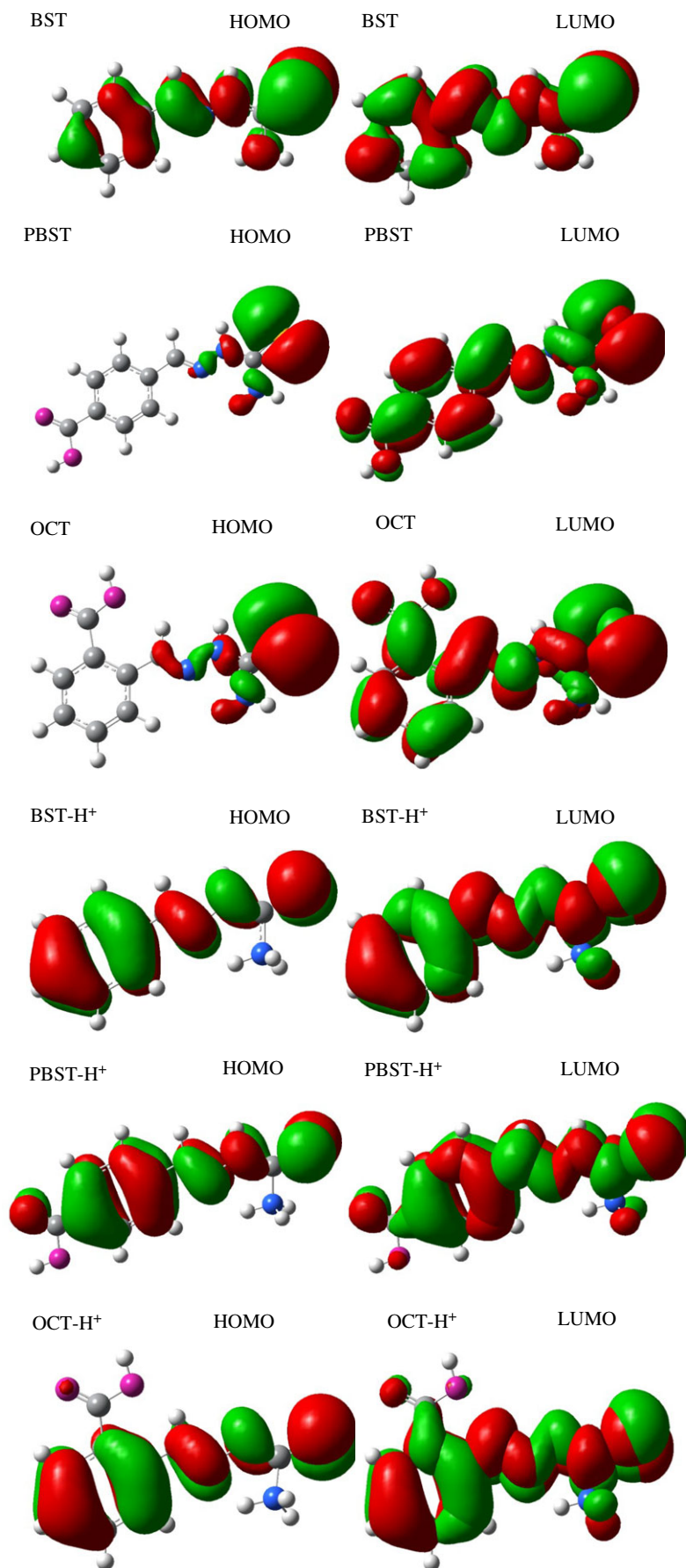


Figure 12. Frontier molecule orbital density distributions of these inhibitors and the protonated forms.

Table 10. Theoretical parameters of BST, PBST and OCT inhibitor and the protonated forms.

parameters	BST	PBST	OCT	BST-H ⁺	PBST-H ⁺	OCT-H ⁺
E_{HOMO} (eV)	-5.9772	-6.1944	-6.0986	-10.1295	-10.3085	-10.3322
E_{LUMO} (eV)	-2.1490	-2.7433	-2.5512	-6.2983	-6.5176	-6.4123
ΔE (eV)	3.8282	3.4511	3.5474	3.8312	3.7909	3.9199
μ (D)	5.4560	3.1922	4.3649	4.3037	10.8639	9.4524
I (eV)	5.9772	6.1944	6.0986	10.1295	10.3085	10.3322
A (eV)	2.1490	2.7433	2.5512	6.2983	6.5176	6.4123
χ (eV)	4.0631	4.4689	4.3249	8.2139	8.4131	8.3722
ρ (eV)	1.9141	1.7256	1.7737	1.9156	1.8954	1.9599
σ [(eV) ⁻¹]	0.5224	0.5795	0.5638	0.5220	0.5276	0.5102

$$\rho = \frac{I - A}{2} \quad (3.8)$$

and

$$\sigma = \frac{1}{\rho}. \quad (3.9)$$

All of these calculated quantum chemical parameters are summarized in table 10. It is apparent that the neutral form of PBST inhibitor as well as its protonated form PBST-H⁺ has a minimum value of E_{LUMO} and lowest value of ΔE which is well in agreement with its highest inhibition efficiency. Moreover, PBST inhibitor shows the lowest value of dipole moment (μ), which will favour accumulation of the inhibitor [66]. However, there is still a controversy about the correlation between the dipole moment and inhibition efficiency that many researchers suggested that the inhibition efficiency increased with the increase of dipole moment [67,68], while others stated that inhibitor molecule with a lower value of dipole moment revealed higher inhibition efficiency [66]. Generally, the value of electronegativity χ represents the chemical potential and a higher value indicates better inhibition performance. In addition, an inhibitor always shows a higher inhibition efficiency when the value of global hardness is smaller according to the hard-soft acid base (HSAB) principle [69]. Inspection of table 10 also demonstrates that PBST has the highest electronegativity and lowest global hardness, resulting in the maximum inhibition efficiency compared to the other two inhibitors, which is consistent with the result of weight loss and electrochemical measurements.

4. Conclusion

Gravimetric measurements, polarization curves, electrochemical impedance spectroscopy and scanning electron microscopy (SEM) were used to study the inhibition behaviour of three new benzaldehyde thiosemicarbazone derivatives for mild steel in 0.5 M H₂SO₄ solution. Results revealed that all these compounds are good inhibitors for Q235 steel in 0.5 M H₂SO₄ solution and PBST inhibitor showed the maximum inhibition efficiency of 96.6% at 300 μ M. The inhibition efficiency increases with increasing inhibitors concentration and temperature. The results of polarization curves indicated that these three compounds behaved as mixed type and PBST and OCT predominantly anodic. The adsorption of these inhibitors on Q235 steel surface was according to Langmuir adsorption isotherm. The results of theoretical calculation and SEM studies were found to be in good agreement with that of weight loss and electrochemical measurements.

Data accessibility. The datasets generated in this work are available from the corresponding author on reasonable request. Our data are available from the Dryad Digital Repository: <https://doi.org/10.5061/dryad.7cn76k3> [70].

Authors' contributions. H.H.Z. performed the measurements. Y.C. wrote the manuscript. Z.Z. supervised and interpreted the research. C.K.Q. helped us revise the manuscript and performed the theoretical calculations. All authors discussed the results and commented on the manuscript. All authors have read and approved the manuscript before submission. Competing interests. The authors declare no competing interests.

Funding. The authors wish to acknowledge the financial support of the National Natural Science Foundation of China (Project 21403194, 51771173), the Natural Science Foundation of Shandong Province (ZR2019QEM003, ZR2014BQ027, ZR2016BP11), the Project of Focus on Research and Development Plan in Shandong Province (2019GSF111048), the Major Project of Binzhou University (2017ZDL02) and Scientific Research Fund of Binzhou University (BZXYLG1904, BZXYFB20140805, BZXYL1403).

Acknowledgements. The authors would like to thank Zhongnian Yang, Yuanwei Liu and Junying Yin (Binzhou University) for their kind help.

References

- Mallaiya K, Subramanian R, Srikanth SS, Gowri S, Rajasekaran N, Selvaraj A. 2011 Electrochemical characterization of the protective film formed by the unsymmetrical Schiff's base on the mild steel surface in acid media. *Electrochim. Acta* **56**, 3857–3863. (doi:10.1016/j.electacta.2011.02.036)
- Daoud D, Douadi T, Hamani H, Chafaa S, Al-Noaimi M. 2015 Corrosion inhibition of mild steel by two new S-heterocyclic compounds in 1 M HCl: experimental and computational study. *Corros. Sci.* **94**, 21–37. (doi:10.1016/j.corsci.2015.01.025)
- Negma NA, Kandile NG, Badr EA, Mohammed MA. 2012 Gravimetric and electrochemical evaluation of environmentally friendly nonionic corrosion inhibitors for carbon steel in 1 M HCl. *Corros. Sci.* **65**, 94–103. (doi:10.1016/j.corsci.2012.08.002)
- Badr GE. 2009 The role of some thiosemicarbazide derivatives as corrosion inhibitors for C-steel in acidic media. *Corros. Sci.* **51**, 2529–2536. (doi:10.1016/j.corsci.2009.06.017)
- Ahamad I, Prasad R, Quraishi MA. 2010 Inhibition of mild steel corrosion in acid solution by Pheniramine drug: experimental and theoretical study. *Corros. Sci.* **52**, 3033–3041. (doi:10.1016/j.corsci.2010.05.022)
- Obot IB, Obi-Egbedi NO. 2010 Adsorption properties and inhibition of mild steel corrosion in sulphuric acid solution by ketoconazole: experimental and theoretical investigation. *Corros. Sci.* **52**, 198–204. (doi:10.1016/j.corsci.2009.09.002)
- Zheng X, Zhang S, Li W, Gong M, Yin L. 2015 Experimental and theoretical studies of two imidazolium-based ionic liquid as inhibitors for mild steel in sulfuric acid solution. *Corros. Sci.* **95**, 168–179. (doi:10.1016/j.corsci.2015.03.012)
- Zakaria K, Hamdy A, Abbas MA, Abo-Elenien OM. 2016 New organic compounds based on siloxane moiety as corrosion inhibitors for carbon steel in HCl solution: weight loss, electrochemical and surface studies. *J. Taiwan Inst. Chem. Eng.* **65**, 530–543. (doi:10.1016/j.jtice.2016.05.036)
- Lashgari M, Malek AM. 2010 Fundamental studies of aluminum corrosion in acidic and basic environments: theoretical predictions and experimental observations. *Electrochim. Acta* **55**, 5253–5257. (doi:10.1016/j.electacta.2010.04.054)
- Thirumalairaj B, Jaganathan M. 2016 Corrosion protection of mild steel by a new binary inhibitor system in hydrochloric acid solution. *Egypt. J. Petrol.* **25**, 423–432.
- Goulart CM, Esteves-Souza A, Martinez-Huitle CA, Rodrigues CJF, Maciel MAM, Echevarria A. 2013 Experimental and theoretical evaluation of semicarbazones and thiosemicarbazones as organic corrosion inhibitors. *Corros. Sci.* **67**, 281–291. (doi:10.1016/j.corsci.2012.10.029)
- Chen S, Kar T. 2012 Theoretical investigation of inhibition efficiencies of some Schiff bases as corrosion inhibitors of aluminum. *Int. J. Electrochem. Sci.* **7**, 6265–6275.
- Benali O, Larabi L, Traisnel M, Gengembra L, Harek Y. 2007 Electrochemical, theoretical and XPS studies of 2-mercapto-1-methylimidazole adsorption on carbon steel in 1 M HClO₄. *Appl. Surf. Sci.* **253**, 6130–6139. (doi:10.1016/j.apsusc.2007.01.075)
- Abd El-raouf M, El-Azabawy OE, El-Azabawy RE. 2015 Investigation of adsorption and inhibitive effect of acid red GRE (183) dye on the corrosion of carbon steel in hydrochloric acid media. *Egypt. J. Petrol.* **24**, 233–239.
- Verma CB, Quraishi MA, Singh A. 2015 2-Aminobenzene-1,3-dicarbonitriles as green corrosion inhibitor for mild steel in 1 M HCl: electrochemical, thermodynamic, surface and quantum chemical investigation. *J. Taiwan Inst. Chem. Eng.* **49**, 229–239. (doi:10.1016/j.jtice.2014.11.029)
- Xia G, Jiang X, Zhou L, Liao Y, Duan M, Wang H, Pu Q, Zhou J. 2015 Synergic effect of methyl acrylate and N-cetylpyridinium bromide in N-cetyl-3-(2-methoxy carbonylvinyl) pyridinium bromide molecule for X70 steel protection. *Corros. Sci.* **94**, 224–236. (doi:10.1016/j.corsci.2015.02.005)
- Ji Y, Xu B, Gong W, Zhang X, Jin X, Ning W, Meng Y, Yang W, Chen Y. 2016 Corrosion inhibition of a new Schiff base derivative with two pyridine rings on Q235 mild steel in 1.0 M HCl. *J. Taiwan Inst. Chem. Eng.* **66**, 301–312. (doi:10.1016/j.jtice.2016.07.007)
- Amin MA, Abd El-Rehim SS, El-Sherbini EEF, Bayoumi RS. 2007 The inhibition of low carbon steel corrosion in hydrochloric acid solutions by succinic acid: Part I. Weight loss, polarization, EIS, PZC, EDX and SEM studies. *Electrochim. Acta* **52**, 3588–3600. (doi:10.1016/j.electacta.2006.10.019)
- Gowraraju ND, Jagadeesan S, Ayyasamy K, Olasunkanmi LO, Ebenso EE, Subramanian C. 2017 Adsorption characteristics of Iota-carrageenan and Inulin biopolymers as potential corrosion inhibitors at mild steel/sulphuric acid interface. *J. Mol. Liq.* **232**, 9–19. (doi:10.1016/j.molliq.2017.02.054)
- Mendonca GLF, Costa SN, Freire VN, Casciano PNS, Correia AN, de Lima-Neto P. 2017 Understanding the corrosion inhibition of carbon steel and copper in sulphuric acid medium by amino acids using electrochemical techniques allied to molecular modeling methods. *Corros. Sci.* **115**, 41–55. (doi:10.1016/j.corsci.2016.11.012)
- Salarvand Z, Amirnasr M, Talebian M, Raeissi K, Meghdadi S. 2017 Enhanced corrosion resistance of mild steel in 1 M HCl solution by trace amount of 2-phenyl-benzothiazole derivatives: experimental, quantum chemical calculations and molecular dynamics (MD) simulation studies. *Corros. Sci.* **114**, 133–145. (doi:10.1016/j.corsci.2016.11.002)
- Muralisankar M, Sreedharan R, Sujith S, Bhuvanesh NSP, Srekanth A. 2017 N(1)-pentyl isatin-N(4)-methyl-N(4)-phenyl thiosemicarbazone (PITSc) as a corrosion inhibitor on mild steel in HCl. *J. Alloys Compd.* **695**, 171–182. (doi:10.1016/j.jallcom.2016.10.173)
- Ghazoui A, Benchat N, El-Hajjaji F, Taleb M, Rais Z, Saddik R, Elaataoui A, Hammouti B. 2017 The study of the effect of ethyl (6-methyl-3-oxopyridazin-2-yl) acetate on mild steel corrosion in 1 M HCl. *J. Alloys Compd.* **693**, 510–517. (doi:10.1016/j.jallcom.2016.09.191)
- Tao Z, Zhang S, Li W, Hou B. 2009 Corrosion inhibition of mild steel in acidic solution by some oxo-triazole derivatives. *Corros. Sci.* **51**, 2588–2595. (doi:10.1016/j.corsci.2009.06.042)
- Bouanis M, Tourabi M, Nyassi A, Zarrouk A, Jama C, Bentiss F. 2016 Corrosion inhibition performance of 2,5-bis(4-dimethylaminophenyl)-1,3,4-oxadiazole for carbon steel in HCl solution, Gravimetric, electrochemical and XPS studies. *Appl. Surf. Sci.* **389**, 952–966. (doi:10.1016/j.apsusc.2016.07.115)
- Mobin M, Rizvi M. 2017 Polysaccharide from *Plantago* as a green corrosion inhibitor for carbon steel in 1 M HCl solution. *Carbohydr. Polym.* **160**, 172–183. (doi:10.1016/j.carbpol.2016.12.056)
- Gece G. 2008 The use of quantum chemical methods in corrosion inhibitor studies. *Corros. Sci.* **50**, 2981–2992. (doi:10.1016/j.corsci.2008.08.043)
- Issaadi S, Douadi T, Chafaa S. 2014 Adsorption and inhibitive properties of a new heterocyclic furan Schiff base on corrosion of copper in HCl

- 1 M: experimental and theoretical investigation. *Appl. Surf. Sci.* **316**, 582–589. (doi:10.1016/j.apsusc.2014.08.050)
29. Torres VV, Rayol VA, Magalhaes M, Viana GM, Aguiar LCS, Machado SP, Orofino H, Elia ED. 2014 Study of thioureas derivatives synthesized from a green route as corrosion inhibitors for mild steel in HCl solution. *Corros. Sci.* **79**, 108–118. (doi:10.1016/j.corsci.2013.10.032)
30. Arab ST. 2008 Inhibition action of thiosemicabazone and some of its ρ -substituted compounds on the corrosion of iron-base metallic glass alloy in 0.5 M H₂SO₄ at 30 °C. *Mater. Res. Bull.* **43**, 510–521. (doi:10.1016/j.materresbull.2007.10.025)
31. Khandani M, Sedaghat T, Erfani N, Haghshenas MR, Khavasi HR. 2013 Synthesis, spectroscopic characterization, structural studies and antibacterial and antitumor activities of diorganotin complexes with 3-methoxysalicylaldehyde thiosemicarbazone. *J. Mol. Struct.* **1037**, 136–143. (doi:10.1016/j.molstruc.2012.12.061)
32. Geethamani P, Kasthuri PK. 2016 The inhibitory action of expired asthalin drug on the corrosion of mild steel in acidic media: a comparative study. *J. Taiwan Inst. Chem. Eng.* **63**, 490–499. (doi:10.1016/j.jtice.2016.03.008)
33. Lee C, Yang W, Parr RG. 1988 Development of the Colle-Salvetti correlation-energy formula into a functional of the electron density. *Phys. Rev. B* **37**, 785–789. (doi:10.1103/PhysRevB.37.785)
34. Musa AY, Kadhum AAH, Mohamad AB, Takriff MS, Kamarudin SK. 2010 On the inhibition of mild steel corrosion by 4-amino-5-phenyl-4H-1,2,4-triazole-3-thiol. *Corros. Sci.* **52**, 526–533. (doi:10.1016/j.corsci.2009.10.009)
35. Jamal Abdu Nasser A, Anwar Sathiq M. 2016 N-[Morpholin-4-yl (phenyl) methyl] acetamide as corrosion inhibitor for mild steel in hydrochloric acid medium. *Arab. J. Chem.* **9**, S691–S698.
36. Satapathy AK, Gunasekaran G, Sahoo SC, Amit K, Rodrigues PV. 2009 Corrosion inhibition by *Justicia gendarussa* plant extract in hydrochloric acid solution. *Corros. Sci.* **51**, 2848–2856. (doi:10.1016/j.corsci.2009.08.016)
37. Abd El Rehim SS, Ibrahim MAM, Khalid KF. 2001 The inhibition of 4-(2'-amino-5'-methylphenylazo) antipyrine on corrosion of mild steel in HCl solution. *Mater. Chem. Phys.* **70**, 268–273. (doi:10.1016/S0254-0584(00)00462-4)
38. Issaadi S, Douadi T, Zouaoui A, Chafaa S, Khan MA, Bouet G. 2011 Novel thiophene symmetrical Schiff base compounds as corrosion inhibitor for mild steel in acidic media. *Corros. Sci.* **53**, 1484–1488. (doi:10.1016/j.corsci.2011.01.022)
39. Li X, Deng S, Fu H. 2011 Triazolyl blue tetrazolium bromide as a novel corrosion inhibitor for steel in HCl and H₂SO₄ solutions. *Corros. Sci.* **53**, 302–309. (doi:10.1016/j.corsci.2010.09.036)
40. Hosseini M, Mertens SFL, Ghorbani M, Arshadi MR. 2003 Asymmetrical Schiff bases as inhibitors of mild steel corrosion in sulphuric acid media. *Mater. Chem. Phys.* **78**, 800–808. (doi:10.1016/S0254-0584(02)00390-5)
41. Khaled KF, Hackerman N. 2004 Ortho-substituted anilines to inhibit copper corrosion in aerated 0.5 M hydrochloric acid. *Electrochim. Acta* **49**, 485–495. (doi:10.1016/j.electacta.2003.09.005)
42. Zhang K, Xu B, Yang W, Yin X, Liu Y, Chen Y. 2015 Halogen-substituted imidazoline derivatives as corrosion inhibitors for mild steel in hydrochloric acid solution. *Corros. Sci.* **90**, 284–295. (doi:10.1016/j.corsci.2014.10.032)
43. Solmaz R, Kardas G, Culha M, Yazici B, Erbil M. 2008 Investigation of adsorption and inhibitive effect of 2-mercaptothiazoline on corrosion of mild steel in hydrochloric acid media. *Electrochim. Acta* **53**, 5941–5952. (doi:10.1016/j.electacta.2008.03.055)
44. Nam ND, Bui QV, Mathesh M, Tan MYJ, Forsyth M. 2013 A study of 4-carboxyphenylboronic acid as a corrosion inhibitor for steel in carbon dioxide containing environments. *Corros. Sci.* **76**, 257–266. (doi:10.1016/j.corsci.2013.06.048)
45. Hazwan Hussin M, Jain Kassim M, Razali NN, Dahon NH, Nasshorudin D. 2016 The effect of *Tinospora crista* extracts as a natural mild steel corrosion inhibitor in 1 M HCl solution. *Arab. J. Chem.* **9**, S616–S624.
46. Zarrouk A, Hammouti B, Lakhilfi T, Traisnel M, Yezin H, Bentiss F. 2015 New 1H-pyrrole-2,5-dione derivatives as efficient organic inhibitors of carbon steel corrosion in hydrochloric acid medium: electrochemical, XPS and DFT studies. *Corros. Sci.* **90**, 572–584. (doi:10.1016/j.corsci.2014.10.052)
47. Ahamad I, Prasad R, Quraishi M. 2010 Experimental and quantum chemical characterization of the adsorption of some Schiff base compounds of phthaloyl thiocarbonylhydrazide on the mild steel in acid solutions. *Mater. Chem. Phys.* **124**, 1155–1165. (doi:10.1016/j.matchemphys.2010.08.051)
48. Aljourani J, Raeissi K, Golzar M. 2009 Benzimidazole and its derivatives as corrosion inhibitors for mild steel in 1 M HCl solution. *Corros. Sci.* **51**, 1836–1843. (doi:10.1016/j.corsci.2009.05.011)
49. Chevalier M, Robert F, Amusant N, Traisnel M, Roos C, Lebrini M. 2014 Enhanced corrosion resistance of mild steel in 1 M hydrochloric acid solution by alkaloids extract from *Aniba rosaeodora* plant; electrochemical, phytochemical and XPS studies. *Electrochim. Acta* **131**, 96–105. (doi:10.1016/j.electacta.2013.12.023)
50. Gopal Ji S, Anjum SS, Prakash R. 2015 *Musa paradisiaca* peel extract as green corrosion inhibitor for mild steel in HCl solution. *Corros. Sci.* **90**, 107–117. (doi:10.1016/j.corsci.2014.10.002)
51. Deyab MA. 2016 Corrosion inhibition of aluminum in biodiesel by ethanol extracts of Rosemary leaves. *J. Taiwan Inst. Chem. Eng.* **58**, 536–541. (doi:10.1016/j.jtice.2015.06.021)
52. Behpour M, Ghoreishi SM, Soltani N, Salavati-Niasari M, Hamadani M, Gandomi A. 2008 Electrochemical and theoretical investigation on the corrosion inhibition of mild steel by thiosalicylaldehyde derivatives in hydrochloric acid solution. *Corros. Sci.* **50**, 2172–2181. (doi:10.1016/j.corsci.2008.06.020)
53. Deyab MA. 2015 Egyptian licorice extract as a green corrosion inhibitor for copper in hydrochloric acid solution. *J. Ind. Eng. Chem.* **22**, 384–389. (doi:10.1016/j.jiec.2014.07.036)
54. Abd El-Lateef HM, Abu-Dief AM, Abdel-Rahman LH, Sanudo EC, Aliaga-Alcalde N. 2015 Electrochemical and theoretical quantum approaches on the inhibition of C1018 carbon steel corrosion in acidic medium containing chloride using some newly synthesized phenolic Schiff bases compounds. *J. Electroanal. Chem.* **743**, 120–133. (doi:10.1016/j.jelechem.2015.02.023)
55. Oguzie EE, Unaegbu C, Oguke CE, Okolue BN, Onuchukwu AI. 2004 Inhibition of mild steel corrosion in sulphuric acid using indigo dye and synergistic halide additives. *Mater. Chem. Phys.* **84**, 363–368. (doi:10.1016/j.matchemphys.2003.11.027)
56. Ammar IA, El Khorafi FM. 1973 Adsorbability of thiourea on iron cathodes. *Mater. Corros.* **24**, 702–707. (doi:10.1002/maco.19730240806)
57. Umoren SA, Ebenso EE, Okafor PC. 2007 Effect of halide ions on the corrosion inhibition of aluminium in alkaline medium using polyvinyl alcohol. *J. Appl. Polym. Sci.* **103**, 2810–2816. (doi:10.1002/app.25446)
58. Fouda AS, Al-Sarawy AA, El-Katori EE. 2006 Pyrazolone derivatives as corrosion inhibitors for C-steel in hydrochloric acid solution. *Desalination* **201**, 1–13. (doi:10.1016/j.desal.2006.03.519)
59. Khadom AA, Yaro AS, Amir A, Kadum H. 2010 Corrosion inhibition by naphthylamine and phenylenediamine for the corrosion of copper-nickel alloy in hydrochloric acid. *J. Taiwan Inst. Chem. Eng.* **41**, 122–125. (doi:10.1016/j.jtice.2009.08.001)
60. Martinez S. 2003 Inhibitory mechanism of mimosa tannin using molecular modeling and substitution adsorption isotherms. *Mater. Chem. Phys.* **77**, 97–102. (doi:10.1016/S0254-0584(01)00569-7)
61. Abdallah M. 2002 Rhodanine azosulpha drugs as corrosion inhibitors for corrosion of 304 stainless steel in hydrochloric acid solution. *Corros. Sci.* **44**, 717–728. (doi:10.1016/S0010-938X(01)00100-7)
62. Xia S, Qiu M, Yu L, Liu F, Zhao H. 2008 Molecular dynamics and density functional theory study on relationship between structure of imidazoline derivatives and inhibition performance. *Corros. Sci.* **50**, 2021–2029. (doi:10.1016/j.corsci.2008.04.021)
63. Arslan T, Kandemirli F, Ebenso EE, Love I, Alemu H. 2009 Quantum chemical studies on the corrosion inhibition of some sulphonamides on mild steel in acidic medium. *Corros. Sci.* **51**, 35–47. (doi:10.1016/j.corsci.2008.10.016)
64. Tian H, Li W, Cao K, Hou B. 2013 Potent inhibition of copper corrosion in neutral chloride media by novel non-toxic thiadiazole derivatives. *Corros. Sci.* **73**, 281–291. (doi:10.1016/j.corsci.2013.04.017)
65. Hegazy MA, Badawi AM, Abd El Rehim SS, Kamel WM. 2013 Corrosion inhibition

- of carbon steel using novel N-(2-(2-mercaptoacetoxy)ethyl)-N,N-dimethyl dodecan-1-aminium bromide during acid pickling. *Corros. Sci.* **69**, 110–122. (doi:10.1016/j.corsci.2012.11.031)
66. Khalil N. 2003 Quantum chemical approach of corrosion inhibition. *Electrochim. Acta* **48**, 2635–2640. (doi:10.1016/S0013-4686(03)00307-4)
67. Qurashi MA, Sardar R. 2003 Hector bases: a new class of heterocyclic corrosion inhibitors for mild steel in acid solutions. *J. Appl. Electrochem.* **33**, 1163–1168. (doi:10.1023/B:JACH.0000003865.08986.fb)
68. Khaled KF, Kbabic-Samardžiji N, Hackeman N. 2005 Theoretical study of the structural effects of polymethylene amines on corrosion inhibition of iron in acid solutions. *Electrochim. Acta* **50**, 2515–2520. (doi:10.1016/j.electacta.2004.10.079)
69. Herrag L, Hammouti B, Elkadiri S, Aouniti A, Jama C, Vezin H, Bentiss F. 2010 Adsorption properties and inhibition of mild steel corrosion in hydrochloric solution by some newly synthesized diamine derivatives: experimental and theoretical investigations. *Corros. Sci.* **52**, 3042–3051. (doi:10.1016/j.corsci.2010.05.024)
70. Zhang HH, Qin CK, Chen Y, Zhang Z. 2019 Data from: Inhibition behaviour of mild steel by three new benzaldehyde thiosemicarbazone derivatives in 0.5 M H₂SO₄: experimental and computational study. Dryad Digital Repository. (doi:10.5061/dryad.7cn76k3)